



Brief paper

Synchronization of coupled harmonic oscillators with local interaction[☆]Wei Ren^{*}

Department of Electrical & Computer Engineering, Utah State University, United States

ARTICLE INFO

Article history:

Received 20 October 2007

Received in revised form

13 March 2008

Accepted 23 May 2008

Available online 7 November 2008

Keywords:

Synchronization

Coupled harmonic oscillators

Multi-agent systems

Local interaction

Coordination

ABSTRACT

This paper studies synchronization of coupled second-order linear harmonic oscillators with local interaction. We analyze convergence conditions over, respectively, directed fixed and switching network topologies by using tools from algebraic graph theory, matrix theory, and nonsmooth analysis. It is shown that the coupled harmonic oscillators can be synchronized under mild network connectivity conditions. Examples are given to validate the convergence conditions. The theoretical result is also applied to synchronized motion coordination of multi-agent systems as a proof of concept.

© 2008 Elsevier Ltd. All rights reserved.

1. Introduction

When two objects of mass m are connected by a damper with coefficient b and are each attached to fixed supports by identical springs with spring constants k , they can be represented by

$$m\ddot{x}_1 + kx_1 + b(\dot{x}_1 - \dot{x}_2) = 0 \quad (1a)$$

$$m\ddot{x}_2 + kx_2 + b(\dot{x}_2 - \dot{x}_1) = 0, \quad (1b)$$

where $x_i \in \mathbb{R}$ denotes the position of the i th object. Motivated by (1), we study in this paper n coupled harmonic oscillators with local interaction of the form

$$\ddot{x}_i + \alpha(t)x_i + \sum_{j=1}^n a_{ij}(t)(\dot{x}_i - \dot{x}_j) = 0, \quad i = 1, \dots, n, \quad (2)$$

where $x_i \in \mathbb{R}$ is the position of the i th oscillator, $\alpha(t)$ is a positive gain at time t , and $a_{ij}(t)$ characterizes interaction between oscillators i and j at time t (i.e., $a_{ij}(t) > 0$ if oscillator i can obtain the velocity of oscillator j at time t and $a_{ij}(t) = 0$ otherwise). While (2) conceptually represents a system where n virtual masses are connected by virtual dampers, the purpose of this paper is

to adopt (2) as a distributed algorithm for synchronization of the positions and velocities of n networked point-mass agents.

Synchronization phenomena are common in nature (see Ni-jmeijer and Rodriguez-Angeles (2003) and references therein). An important avenue of study in synchronization focuses on coupled oscillators. One classical example is the Kuramoto model (Kuramoto, 1984), which assumes full connectivity of the network. Recent works generalize the Kuramoto model to nearest neighbor interaction (see e.g., Chopra and Spong (2005), Jadbabaie, Motee, and Barahona (2004) and Papachristodoulou and Jadbabaie (2005)). In the context of multi-agent systems, Paley, Leonard, and Sepulchre (2005, 2006) study connections between phase models of coupled oscillators and kinematic models of self-propelled particle groups and provide feedback control laws that stabilize symmetric formations of multiple, unit speed particles on closed curves. In Chopra and Spong (2006), output synchronization is studied for general passive systems, which unifies several existing results in the literature. In contrast to Chopra and Spong (2005, 2006), Jadbabaie et al. (2004), Paley et al. (2005), Papachristodoulou and Jadbabaie (2005) and Paley et al. (2006), algorithm (2) describes coupled second-order linear harmonic oscillators. In particular, the oscillators studied in Paley et al. (2005, 2006) are modeled as points on a torus, whereas the oscillator models studied in this paper are represented by points on a real line. In addition, the linear structure of (2) allows us to derive a milder convergence condition than that in Chopra and Spong (2006) and explicitly show the final trajectories to which each oscillator converges over directed fixed network topologies.

Related to synchronization are consensus problems in multi-agent systems. Consensus means that a team of agents reaches an agreement on a common value by negotiating with their neighbors

[☆] This paper was not presented at any IFAC meeting. This paper was recommended for publication in revised form by Associate Editor Masayuki Fujita under the direction of Editor Ian R. Petersen. This work was supported in part by a National Science Foundation CAREER Award (ECCS-0748287).

^{*} Corresponding address: Department of Electrical and Computer Engineering, Utah State University, 4120 Old Main Hill, 84322-4120 Logan, UT, United States. Tel.: +1 435 797 2831; fax: +1 435 797 3054.

E-mail address: wren@engineering.usu.edu.

(see Olfati-Saber, Fax, and Murray (2007) and Ren, Beard, and Atkins (2007) for recent surveys). In particular, (2) is related to the second-order consensus-type algorithms studied in Ren and Atkins (2007), Tanner, Jadbabaie, and Pappas (2007) and Xie and Wang (2007). In Tanner et al. (2007), flocking behavior is analyzed using nonsmooth analysis over undirected fixed and switching network topologies. Ren and Atkins (2007) proposes and analyzes consensus algorithms for double-integrator dynamics and shows that unlike the single-integrator case, both the network topology and the coupling strength of relative velocities between neighbors affect the convergence result in the general case of directed interaction. In addition, Xie and Wang (2007) studies a consensus algorithm for double-integrator dynamics where a damping term for the velocities is introduced and analyzes the algorithm over an undirected network topology. However, in contrast to the algorithms in Ren and Atkins (2007), Tanner et al. (2007) and Xie and Wang (2007), where the consensus equilibrium for the velocities is a nonzero constant or zero, the positions and velocities using (2) are synchronized to achieve oscillatory motions.

The objective of the current paper is to analyze convergence conditions for (2) over, respectively, directed fixed and switching network topologies. The convergence analysis will be conducted by using tools from algebraic graph theory, matrix theory, and nonsmooth analysis. The theoretical result is also applied to synchronized motion coordination of multi-agent systems as a proof of concept.

2. Background

To analyze the convergence conditions for coupled harmonic oscillators over directed fixed and switching network topologies, we use *directed graph* $\mathcal{G} = (\mathcal{V}, \mathcal{E})$, where $\mathcal{V} = \{1, \dots, n\}$ is the *node set* and $\mathcal{E} \subseteq \mathcal{V} \times \mathcal{V}$ is the *edge set*, to model interaction among n oscillators. Let $\mathcal{A} = [a_{ij}] \in \mathbb{R}^{n \times n}$ be the *adjacency matrix* associated with \mathcal{G} . Adjacency matrix \mathcal{A} is defined such that a_{ij} is a positive weight if $(j, i) \in \mathcal{E}$, while $a_{ij} = 0$ if $(j, i) \notin \mathcal{E}$. Note that for directed graphs, \mathcal{A} is not necessarily symmetric. Also note that $a_{ij}(t)$ in (2) is the (i, j) entry of \mathcal{A} at time t . Let (*nonsymmetric*) *Laplacian matrix* $\mathcal{L} = [\ell_{ij}] \in \mathbb{R}^{n \times n}$ associated with \mathcal{G} be defined as $\ell_{ii} = \sum_{j=1, j \neq i}^n a_{ij}$ and $\ell_{ij} = -a_{ij}$, where $i \neq j$.

A *directed path* of \mathcal{G} is a sequence of edges of the form $(i_1, i_2), (i_2, i_3), \dots$, where $i_j \in \mathcal{V}$. A directed graph is *strongly connected* if there is a directed path from every node to every other node. A directed graph has a *directed spanning tree* if there exists at least one node having a directed path to all other nodes. A directed graph is *balanced* if $\sum_{j=1}^n a_{ij} = \sum_{j=1}^n a_{ji}$, for all i .

Let $r_i = x_i$ and $v_i = \dot{x}_i$. Eq. (2) can be written as

$$\begin{aligned} \dot{r}_i &= v_i, \\ \dot{v}_i &= -\alpha(t)r_i - \sum_{j=1}^n a_{ij}(t)(v_i - v_j), \quad i = 1, \dots, n. \end{aligned} \quad (3)$$

Let $r = [r_1, \dots, r_n]^T$ and $v = [v_1, \dots, v_n]^T$. Eq. (3) can be written in matrix form as

$$\begin{bmatrix} \dot{r} \\ \dot{v} \end{bmatrix} = \underbrace{\begin{bmatrix} 0_n & I_n \\ -\alpha(t)I_n & -\mathcal{L}(t) \end{bmatrix}}_{\mathcal{Q}} \begin{bmatrix} r \\ v \end{bmatrix}, \quad (4)$$

where 0_n denotes the $n \times n$ zero matrix, I_n denotes the $n \times n$ identity matrix, and $\mathcal{L}(t) \in \mathbb{R}^{n \times n}$ is the (*nonsymmetric*) Laplacian matrix associated with directed graph \mathcal{G} at time t .

3. Convergence over directed fixed network topologies

In this section, we consider the convergence of (3) over directed fixed network topologies. Here we assume that both α and \mathcal{L} in (4) are constant. Both leaderless and leader-following cases will be addressed. We need the following lemmas for our main result.

Lemma 3.1 (Ren & Beard, 2005). *Let \mathcal{L} be the (nonsymmetric) Laplacian matrix associated with \mathcal{G} . Then \mathcal{L} has a simple zero eigenvalue and all its other eigenvalues have positive real parts if and only if \mathcal{G} has a directed spanning tree. In addition, there exist $\mathbf{1}_n$, where $\mathbf{1}_n$ is an $n \times 1$ column vector of all ones, satisfying $\mathcal{L}\mathbf{1}_n = 0$ and $\mathbf{p} \in \mathbb{R}^n$ satisfying $\mathbf{p} \geq 0$, $\mathbf{p}^T \mathcal{L} = 0$, and $\mathbf{p}^T \mathbf{1}_n = 1$.*

Lemma 3.2. *Let $\mu_i \in \mathbb{C}$ be the i th eigenvalue of $-\mathcal{L}$. Also let $\chi_{ri} \in \mathbb{C}^n$ and $\chi_{\ell i} \in \mathbb{C}^n$ be, respectively, the right and left eigenvectors of $-\mathcal{L}$ associated with μ_i . Then the eigenvalues of \mathcal{Q} defined in (4) are given by $\lambda_{i\pm} = \frac{\mu_i \pm \sqrt{\mu_i^2 - 4\alpha}}{2}$ with associated right eigenvectors $\varphi_{ri\pm} = [\chi_{ri}^T, \lambda_{i\pm} \chi_{ri}^T]^T$ and left eigenvector $\varphi_{\ell i\pm} = [\chi_{\ell i}^T, -\frac{\lambda_{i\pm}}{\alpha} \chi_{\ell i}^T]^T$.*

Proof. Let λ be an eigenvalue of \mathcal{Q} and $\varphi_r = [x_r^T, y_r^T]^T \in \mathbb{C}^{2n}$ be an associated right eigenvector. Then we get that

$$\begin{bmatrix} 0_n & I_n \\ -\alpha I_n & -\mathcal{L} \end{bmatrix} \begin{bmatrix} x_r \\ y_r \end{bmatrix} = \lambda \begin{bmatrix} x_r \\ y_r \end{bmatrix}. \quad (5)$$

It follows from (5) that

$$y_r = \lambda x_r, \quad (6a)$$

$$-\alpha x_r - \mathcal{L} y_r = \lambda y_r, \quad (6b)$$

Combining (6a) and (6b), gives $-\mathcal{L} x_r = \frac{\lambda^2 + \alpha}{\lambda} x_r$. Suppose that μ is an eigenvalue of $-\mathcal{L}$ with an associated right eigenvector χ_r , it follows that $\frac{\lambda^2 + \alpha}{\lambda} = \mu$ and $x_r = \chi_r$. Therefore, it follows that λ satisfies

$$\lambda^2 - \mu\lambda + \alpha = 0 \quad (7)$$

and $\varphi_r = [\chi_r^T, \lambda \chi_r^T]^T$ according to (6a). Noting that μ_i is the i th eigenvalue of $-\mathcal{L}$ with an associated right eigenvector χ_{ri} , it follows from (7) that the eigenvalues of \mathcal{Q} are given by $\lambda_{i\pm} = \frac{\mu_i \pm \sqrt{\mu_i^2 - 4\alpha}}{2}$ with associated right eigenvectors $\varphi_{ri\pm} = [\chi_{ri}^T, \lambda_{i\pm} \chi_{ri}^T]^T$.

Similarly, let $\varphi_\ell = [x_\ell^T, y_\ell^T]^T \in \mathbb{C}^{2n}$ be a left eigenvector of \mathcal{Q} associated with eigenvalue λ . Then we get that

$$[x_\ell^T, y_\ell^T] \begin{bmatrix} 0_n & I_n \\ -\alpha I_n & -\mathcal{L} \end{bmatrix} = \lambda [x_\ell^T, y_\ell^T]. \quad (8)$$

It follows from (8) that

$$y_\ell^T = -\frac{\lambda}{\alpha} x_\ell^T, \quad (9a)$$

$$x_\ell^T - y_\ell^T \mathcal{L} = \lambda y_\ell^T. \quad (9b)$$

Combining (9a) and (9b), gives $-x_\ell^T \mathcal{L} = \frac{\lambda^2 + \alpha}{\lambda} x_\ell^T$. A similar argument to that of the right eigenvectors shows that the left eigenvectors of \mathcal{Q} associated with $\lambda_{i\pm}$ are $\varphi_{\ell i\pm} = [\chi_{\ell i}^T, -\frac{\lambda_{i\pm}}{\alpha} \chi_{\ell i}^T]^T$. ■

In the leaderless case, we have the following theorem.

¹ That is, $\mathbf{1}_n$ and \mathbf{p} are, respectively, right and left eigenvectors of \mathcal{L} associated with the zero eigenvalue.

Theorem 3.1. Let \mathbf{p} be defined as in Lemma 3.1. Let $\mu_i, \lambda_{i\pm}, \varphi_{r_{i\pm}}$, and $\varphi_{\ell_{i\pm}}$ be defined as in Lemma 3.2. Suppose that directed graph \mathcal{G} has a directed spanning tree. Using (3), $r_i(t) \rightarrow \cos(\sqrt{\alpha}t)\mathbf{p}^T r(0) + \frac{1}{\sqrt{\alpha}} \sin(\sqrt{\alpha}t)\mathbf{p}^T v(0)$ and $v_i(t) \rightarrow -\sqrt{\alpha} \sin(\sqrt{\alpha}t)\mathbf{p}^T r(0) + \cos(\sqrt{\alpha}t)\mathbf{p}^T v(0)$ for large t .

Proof. Note that directed graph \mathcal{G} has a directed spanning tree. It follows from Lemma 3.1 that $-\mathcal{L}$ has a simple zero eigenvalue with an associated right eigenvector $\mathbf{1}_n$ and left eigenvector \mathbf{p} that satisfies $\mathbf{p} \geq 0$, $\mathbf{p}^T \mathcal{L} = 0$, and $\mathbf{p}^T \mathbf{1}_n = 1$. In addition, all other eigenvalues of $-\mathcal{L}$ have negative real parts. Without loss of generality, let $\mu_1 = 0$ and then we get that $\text{Re}(\mu_i) < 0$, $i = 2, \dots, n$, where $\text{Re}(\cdot)$ denotes the real part of a number. Accordingly, it follows from Lemma 3.2 that $\lambda_{1\pm} = \pm\sqrt{\alpha}j$ with associated right and left eigenvectors given by

$$\varphi_{r_{1\pm}} = [\mathbf{1}_n^T, \pm\sqrt{\alpha}j\mathbf{1}_n^T]^T, \quad \varphi_{\ell_{1\pm}} = \left[\mathbf{p}^T, \pm \frac{1}{\sqrt{\alpha}j} \mathbf{p}^T \right]^T, \quad (10)$$

where j is the imaginary unit. Because $\text{Re}(\mu_i) < 0$, $i = 2, \dots, n$, it follows that $\text{Re}(\lambda_{i-}) = \text{Re}(\frac{\mu_i - \sqrt{\mu_i^2 - 4\alpha}}{2}) < 0$, $i = 2, \dots, n$. Noting that $\lambda_{i+} \lambda_{i-} = \alpha$, $i = 2, \dots, n$, it follows that $\arg(\lambda_{i+}) = -\arg(\lambda_{i-})$, where $\arg(\cdot)$ denotes the phase of a number. Therefore, it follows that $\text{Re}(\lambda_{i+}) < 0$, $i = 2, \dots, n$.

Note that \mathcal{Q} can be written in Jordan canonical form as

$$\mathcal{Q} = \underbrace{[w_1, \dots, w_{2n}]_P}_{p} \begin{bmatrix} \sqrt{\alpha}j & 0 & \mathbf{0}_{1 \times (2n-2)} \\ 0 & -\sqrt{\alpha}j & \mathbf{0}_{1 \times (2n-2)} \\ \mathbf{0}_{(2n-2) \times 1} & \mathbf{0}_{(2n-2) \times 1} & \bar{J} \end{bmatrix} \underbrace{\begin{bmatrix} v_1^T \\ \vdots \\ v_{2n}^T \end{bmatrix}}_{p^{-1}}, \quad (11)$$

where $w_i \in \mathbb{R}^{2n}$, $i = 1, \dots, 2n$, can be chosen to be the right eigenvectors or generalized eigenvectors of \mathcal{Q} , $v_i \in \mathbb{R}^{2n}$, $i = 1, \dots, 2n$, can be chosen to be the left eigenvectors or generalized eigenvectors of \mathcal{Q} , and \bar{J} is the Jordan upper diagonal block matrix corresponding to eigenvalues λ_{i+} and λ_{i-} , $i = 2, \dots, n$. Because $P^{-1}P = I_{2n}$, w_i and v_i must satisfy that $v_i^T w_i = 1$ and $v_i^T w_k = 0$, where $i \neq k$. Accordingly, we let $w_1 = \varphi_{r_{1+}}$, $w_2 = \varphi_{r_{1-}}$, $v_1 = \frac{1}{2}\varphi_{\ell_{1+}}$, and $v_2 = \frac{1}{2}\varphi_{\ell_{1-}}$, where $\varphi_{r_{1\pm}}$ and $\varphi_{\ell_{1\pm}}$ are defined in (10).

Note that $\lim_{t \rightarrow \infty} e^{\bar{J}t} \rightarrow 0$. For large t , $e^{\mathcal{Q}t} = P e^{tP^{-1}}$ approaches

$$\begin{aligned} & e^{\sqrt{\alpha}jt} \begin{bmatrix} \mathbf{1}_n \\ \sqrt{\alpha}j\mathbf{1}_n \end{bmatrix} \begin{bmatrix} \frac{1}{2}\mathbf{p}^T, \frac{1}{2\sqrt{\alpha}j}\mathbf{p}^T \\ \frac{1}{2}\mathbf{p}^T, -\frac{1}{2\sqrt{\alpha}j}\mathbf{p}^T \end{bmatrix} \\ & + e^{-\sqrt{\alpha}jt} \begin{bmatrix} \mathbf{1}_n \\ -\sqrt{\alpha}j\mathbf{1}_n \end{bmatrix} \begin{bmatrix} \frac{1}{2}\mathbf{p}^T, \frac{1}{2\sqrt{\alpha}j}\mathbf{p}^T \\ \frac{1}{2}\mathbf{p}^T, -\frac{1}{2\sqrt{\alpha}j}\mathbf{p}^T \end{bmatrix} \\ & = \begin{bmatrix} \cos(\sqrt{\alpha}t)\mathbf{1}_n\mathbf{p}^T & \frac{1}{\sqrt{\alpha}} \sin(\sqrt{\alpha}t)\mathbf{1}_n\mathbf{p}^T \\ -\sqrt{\alpha} \sin(\sqrt{\alpha}t)\mathbf{1}_n\mathbf{p}^T & \cos(\sqrt{\alpha}t)\mathbf{1}_n\mathbf{p}^T \end{bmatrix}. \end{aligned}$$

The solution to (4) is given by $\begin{bmatrix} r(t) \\ v(t) \end{bmatrix} = e^{\mathcal{Q}t} \begin{bmatrix} r(0) \\ v(0) \end{bmatrix}$. Therefore, it follows that $r_i(t) \rightarrow \cos(\sqrt{\alpha}t)\mathbf{p}^T r(0) + \frac{1}{\sqrt{\alpha}} \sin(\sqrt{\alpha}t)\mathbf{p}^T v(0)$ and $v_i(t) \rightarrow -\sqrt{\alpha} \sin(\sqrt{\alpha}t)\mathbf{p}^T r(0) + \cos(\sqrt{\alpha}t)\mathbf{p}^T v(0)$ for large t . ■

Under the condition of Theorem 3.1, all r_i converge to a common oscillatory trajectory, so do all v_i . That is, the n coupled harmonic oscillators are synchronized. We next consider the case where there exists a virtual leader, labeled as oscillator 0 with states r_0 and v_0 .

Suppose that r_0 and v_0 satisfy

$$\dot{r}_0 = v_0, \quad \dot{v}_0 = -\alpha r_0. \quad (12)$$

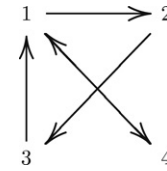


Fig. 1. Directed graph \mathcal{G} in the case of directed fixed network topologies.

In this case, we study the algorithm

$$\begin{aligned} \dot{r}_i &= v_i, \\ \dot{v}_i &= -\alpha r_i - \sum_{j=1}^n a_{ij}(v_i - v_j) - a_{i0}(v_i - v_0), \end{aligned} \quad (13)$$

where $i = 1, \dots, n$ and a_{i0} is a positive constant if v_0 is available to oscillator i and $a_{i0} = 0$ otherwise.

Corollary 3.2. Suppose that the virtual leader has a directed path to all oscillators. Using algorithm (13), $r_i(t) \rightarrow r_0(t)$ and $v_i(t) \rightarrow v_0(t)$ for large t , where $r_0(t) = \cos(\sqrt{\alpha}t)r_0(0) + \frac{1}{\alpha} \sin(\sqrt{\alpha}t)v_0(0)$ and $v_0(t) = -\sqrt{\alpha} \sin(\sqrt{\alpha}t)r_0(0) + \cos(\sqrt{\alpha}t)v_0(0)$.

Proof. It is straightforward to show that the solution to (12) is given by $r_0(t) = \cos(\sqrt{\alpha}t)r_0(0) + \frac{1}{\alpha} \sin(\sqrt{\alpha}t)v_0(0)$ and $v_0(t) = -\sqrt{\alpha} \sin(\sqrt{\alpha}t)r_0(0) + \cos(\sqrt{\alpha}t)v_0(0)$. Consider that the team consists of $n + 1$ oscillators (oscillators 1– n and oscillator 0). The proof is a direct application of that of Theorem 3.1. ■

We also consider the case where there exist deviations between oscillator states. In this case, we study the algorithm

$$\begin{aligned} \dot{r}_i &= v_i, \\ \dot{v}_i &= -\alpha(r_i - \delta_i) - \sum_{j=1}^n a_{ij}(v_i - v_j) - a_{i0}(v_i - v_0), \end{aligned} \quad (14)$$

where $i = 1, \dots, n$ and δ_i is a constant.

Corollary 3.3. Suppose that the virtual leader has a directed path to all oscillators. Using (14), $r_i(t) \rightarrow r_0(t) + \delta_i$ and $v_i(t) \rightarrow v_0(t)$ for large t , where $r_0(t)$ and $v_0(t)$ are defined in Corollary 3.2.

Proof. Let $\tilde{r}_i = r_i - \delta_i$. Noting that $\dot{\tilde{r}}_i = v_i$, it follows from Corollary 3.2 that $\tilde{r}_i(t) \rightarrow r_0(t)$ and $v_i(t) \rightarrow v_0(t)$ for large t with \tilde{r}_i playing the role of r_i in (13). ■

Example 3.4. To illustrate, we show simulation results involving four coupled harmonic oscillators using (3) over directed fixed network topology \mathcal{G} as shown in Fig. 1. Note that \mathcal{G} in this case has a directed spanning tree, implying that the condition of Theorem 3.1 is satisfied. We assume that $a_{ij} = 1$ if $(j, i) \in \mathcal{E}$ and $a_{ij} = 0$ otherwise. Figs. 2 and 3 show, respectively, the evolution of the oscillator states with $\alpha = 1$ and $\alpha = 4$. Note that the oscillator states are synchronized for both $\alpha = 1$ and $\alpha = 4$. However, the value of α has an effect on the magnitude and frequency of the synchronized states.

4. Convergence over directed switching network topologies

In this section, we consider the convergence of (3) over directed switching network topologies. We consider two cases, namely, (i) directed graph $\mathcal{G}(t)$ is strongly connected and balanced at each time instant; and (ii) directed graph $\mathcal{G}(t)$ has a directed spanning tree at each time instant.

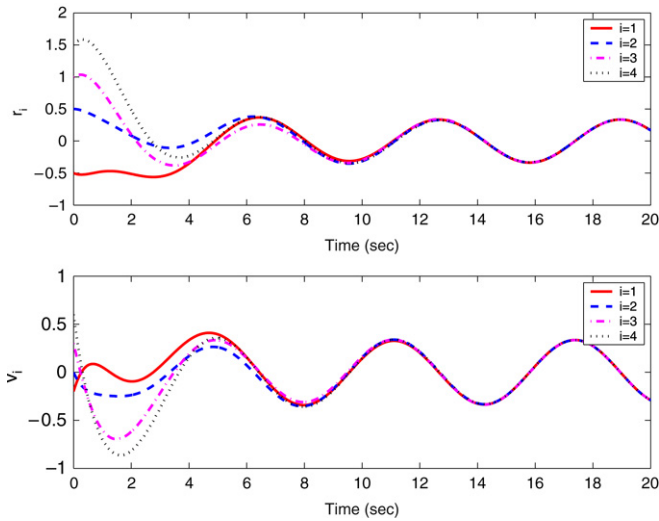


Fig. 2. Evolution of oscillator states over directed fixed network topologies with $\alpha = 1$ and \mathcal{G} shown in Fig. 1.

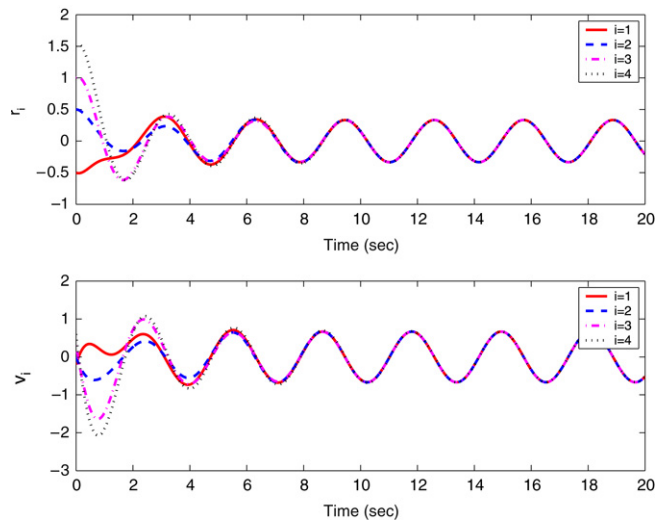


Fig. 3. Evolution of oscillator states over directed fixed network topologies with $\alpha = 4$ and \mathcal{G} shown in Fig. 1.

Let \mathcal{P} denote a set indexing the class of all possible directed graphs \mathcal{G}_p , where $p \in \mathcal{P}$, defined on n nodes. Note that \mathcal{P} is a finite set by definition. Suppose that (3) can be written as

$$\begin{bmatrix} \dot{r} \\ \dot{v} \end{bmatrix} = \underbrace{\begin{bmatrix} 0_n & I_n \\ -\alpha_{\sigma(t)} I_n & -\mathcal{L}_{\sigma(t)} \end{bmatrix}}_{\mathcal{R}_{\sigma(t)}} \begin{bmatrix} r \\ v \end{bmatrix}, \tag{15}$$

where $\sigma : [0, \infty) \rightarrow \mathcal{P}$ is a piecewise constant switching signal with switching times t_0, t_1, \dots , $\alpha_{\sigma(t)}$ is a positive gain associated with directed graph $\mathcal{G}_{\sigma(t)}$, and $\mathcal{L}_{\sigma(t)}$ is the (nonsymmetric) Laplacian matrix associated with directed graph $\mathcal{G}_{\sigma(t)}$.

Theorem 4.1. Suppose that $\sigma(t) \in \mathcal{P}_{sb}$, where $\mathcal{P}_{sb} \subset \mathcal{P}$ denotes the set indexing the class of all possible directed graphs defined on n nodes that are strongly connected and balanced. Also suppose that $\alpha_{\sigma(t)} \equiv \alpha_{sb}$, where α_{sb} is a positive scalar. Using (3), $r_i(t) \rightarrow r_j(t)$ and $v_i(t) \rightarrow v_j(t)$ as $t \rightarrow \infty$.

Proof. The proof is motivated by that of Theorem 1 in Tanner et al. (2007), which relies on differential inclusions and nonsmooth

analysis. We only sketch the main steps of the proof. Consider the Lyapunov function candidate

$$V = \frac{1}{2} \alpha_{sb} r^T r + \frac{1}{2} v^T v. \tag{16}$$

Noting that \dot{v} is discontinuous due to switches of network topologies, we let $\dot{v} \in^{a.e} K[-\mathcal{L}_{\sigma(t)} v] - \alpha_{sb} r$, where $K[\cdot]$ is a differential inclusion and *a.e* denotes “almost everywhere”. The generalized derivative of V is given by $V^\circ = \alpha_{sb} v^T \dot{r} + v^T [-\alpha_{sb} r + \phi_v] = v^T \phi_v$, where ϕ_v is an arbitrary element of $K[-\mathcal{L}_{\sigma(t)} v]$. Note that directed graph $\mathcal{G}_{\sigma(t)}$ is strongly connected and balanced. It follows from Olfati-Saber and Murray (2004) that $-v^T \mathcal{L}_{\sigma(t)} v \leq 0$, which implies that $\max_{\phi_v \in K[-\mathcal{L}_{\sigma(t)} v]} (v^T \phi_v) = \max \overline{\text{co}}(-v^T \mathcal{L}_{\sigma(t)} v) = 0$. In particular, $\max \overline{\text{co}}(-v^T \mathcal{L}_{\sigma(t)} v) = 0$ if and only if $v_i = v_j$, which in turn implies that $\dot{v}_i = \dot{v}_j$. Noting that $\alpha_{\sigma(t)} \equiv \alpha_{sb}$, it follows from (15) (see also (3)) that $r_i = r_j$ when $v_i = v_j$ and $\dot{v}_i = \dot{v}_j$. It thus follows from the invariance principle for differential inclusions (Ryan, 1998) that $r_i(t) \rightarrow r_j(t)$ and $v_i(t) \rightarrow v_j(t)$ as $t \rightarrow \infty$. ■

Let $r_{ij} = r_i - r_j$ and $v_{ij} = v_i - v_j$. Also let $\tilde{r} = [r_{12}, r_{23}, \dots, r_{(n-1)n}]^T$ and $\tilde{v} = [v_{12}, v_{23}, \dots, v_{(n-1)n}]^T$. Eq. (15) can be rewritten as

$$\begin{bmatrix} \dot{\tilde{r}} \\ \dot{\tilde{v}} \end{bmatrix} = \underbrace{\begin{bmatrix} 0_{n-1} & I_{n-1} \\ -\alpha_{\sigma(t)} I_{n-1} & -\mathcal{D}_{\sigma(t)} \end{bmatrix}}_{\mathcal{R}_{\sigma(t)}} \begin{bmatrix} \tilde{r} \\ \tilde{v} \end{bmatrix}, \tag{17}$$

where $\mathcal{D}_{\sigma(t)} \in \mathbb{R}^{(n-1) \times (n-1)}$ can be derived from $\mathcal{L}_{\sigma(t)}$.

Theorem 4.2. Let $\mathcal{P}_{st} \subset \mathcal{P}$ denote the set indexing the class of all possible directed graphs defined on n nodes that have a directed spanning tree. The following two statements hold:

- (1) Matrix \mathcal{R}_p defined in (17) is stable for each $p \in \mathcal{P}_{st}$.
- (2) Let $a_p \geq 0$ and $\chi_p > 0$, for which $\|e^{\mathcal{R}_p t}\| \leq e^{(a_p - \chi_p t)}$, $t \geq 0$. Suppose that $\sigma(t) \in \mathcal{P}_{st}$. If $t_{k+1} - t_k > \sup_{p \in \mathcal{P}_{st}} \{\frac{a_p}{\chi_p}\}$, $\forall k = 0, 1, \dots$, then using (3), $r_i(t) \rightarrow r_j(t)$ and $v_i(t) \rightarrow v_j(t)$ as $t \rightarrow \infty$.

Proof. For the first statement, note that Theorem 3.1 shows that for each $p \in \mathcal{P}_{st}$, $r_i(t) \rightarrow r_j(t)$ and $v_i(t) \rightarrow v_j(t)$ as $t \rightarrow \infty$, which implies that $\tilde{r}(t) \rightarrow 0$ and $\tilde{v}(t) \rightarrow 0$ as $t \rightarrow \infty$. It thus follows from (17) that \mathcal{R}_p is stable for each $p \in \mathcal{P}_{st}$.

For the second statement, under the condition of the theorem, because \mathcal{R}_p is stable for each $p \in \mathcal{P}_{st}$, it follows from Morse (1996, Lemma 2) that switched system (17) is globally exponentially stable if $t_{k+1} - t_k > \sup_{p \in \mathcal{P}_{st}} \{\frac{a_p}{\chi_p}\}$, $\forall k = 0, 1, \dots$. Equivalently, it follows that under the same condition $r_i(t) \rightarrow r_j(t)$ and $v_i(t) \rightarrow v_j(t)$ as $t \rightarrow \infty$. ■

Note that Theorem 4.2 imposes a bound on how fast the network topology can switch while Theorem 4.1 does not. Also note that the convergence condition in Theorem 4.2 is only a sufficient condition. When there exists a virtual leader, the analysis can follow a similar line to that of Theorems 4.1 and 4.2.

Example 4.3. To illustrate, we show simulation results involving four coupled harmonic oscillators using (3) over directed switching network topologies. We first let $\alpha_{\sigma(t)} \equiv 1$ and $\mathcal{G}(t)$ switches randomly from $\{\mathcal{G}_1, \mathcal{G}_2, \mathcal{G}_3\}$ as shown in Fig. 4. We assume that $a_{ij} = 1$ if $(j, i) \in \mathcal{E}$ and $a_{ij} = 0$ otherwise. Here we let $t_0 = 0$ s and choose t_k randomly from $(2k - 2, 2k)$ s, $k = 1, 2, \dots$. Note that $\mathcal{G}_1 - \mathcal{G}_3$ shown in Fig. 4 are all strongly connected and balanced, implying that the condition of Theorem 4.1 is satisfied. Fig. 5 shows the evolution of the oscillator states in this case. Note that all oscillator states are synchronized.

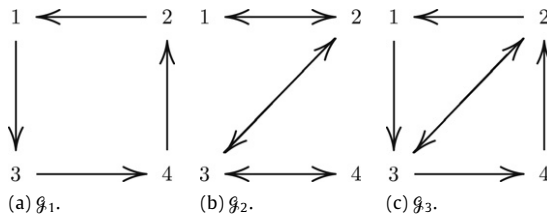


Fig. 4. Directed graphs \mathcal{G}_1 – \mathcal{G}_3 . We assume that $a_{ij} = 1$ if $(j, i) \in \mathcal{E}$ and $a_{ij} = 0$ otherwise. All \mathcal{G}_1 – \mathcal{G}_3 are strongly connected and balanced.

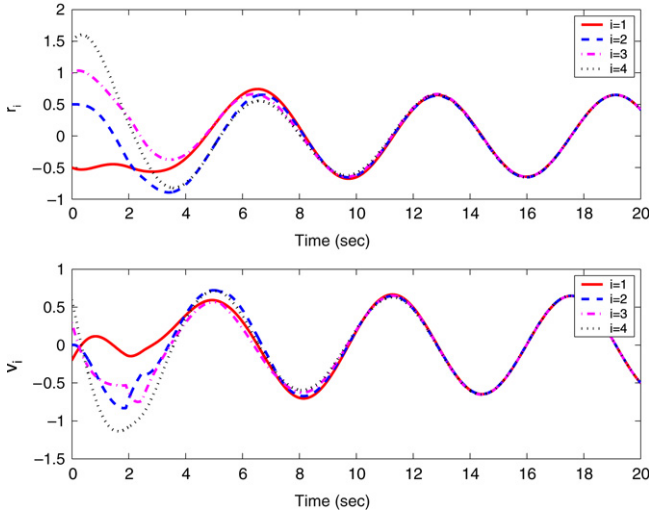


Fig. 5. Evolution of oscillator states over directed switching network topologies when $\alpha_{\sigma(t)} \equiv 1$ and $\mathcal{G}(t)$ switches from $\{\mathcal{G}_1, \mathcal{G}_2, \mathcal{G}_3\}$ as shown in Fig. 4.

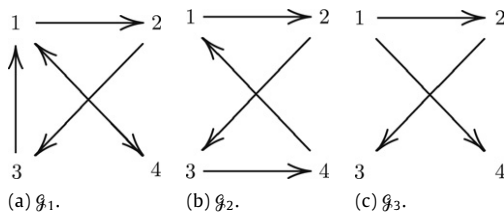


Fig. 6. Directed graphs \mathcal{G}_1 – \mathcal{G}_3 . All of them have a directed spanning tree.

We then let $\alpha_{\sigma(t)}$ switch from $\{\alpha_1, \alpha_2, \alpha_3\}$, where

$$\alpha_1 = 1, \quad \alpha_2 = 4, \quad \alpha_3 = 9 \quad (18)$$

and $\mathcal{G}(t)$ switches randomly from $\{\mathcal{G}_1, \mathcal{G}_2, \mathcal{G}_3\}$ as shown in Fig. 6. Here we again let $t_0 = 0$ s and choose t_k randomly from $(2k - 2, 2k)$ s, $k = 1, 2, \dots$. Note that \mathcal{G}_1 – \mathcal{G}_3 shown in Fig. 6 all have a directed spanning tree, implying that the condition of Theorem 4.2 is satisfied. Fig. 7 shows the evolution of the oscillator states in this case. In contrast to the previous case, the oscillator states do not approach a uniform magnitude and frequency due to switching of α values. However, all oscillator states are still synchronized.

5. Application to motion coordination of multi-agent systems

In this section, we apply algorithm (14) to motion coordination of multi-agent systems. Suppose that there are four point-mass agents in the team with dynamics give by $\dot{p}_i = q_i$ and $\dot{q}_i = w_i$, $i = 1, \dots, 4$, where $p_i = [x_i, y_i]^T$ is the position, $q_i = [v_{xi}, v_{yi}]^T$ is the velocity, and $w_i = [w_{xi}, w_{yi}]^T$ is the acceleration input. Also suppose that there exists a virtual leader with position $p_0 = [x_0, y_0]^T$ and velocity $q_0 = [v_{x0}, v_{y0}]^T$, and p_0 and q_0 satisfy

$$\dot{p}_0 = q_0, \quad \dot{q}_0 = -\alpha p_0, \quad (19)$$

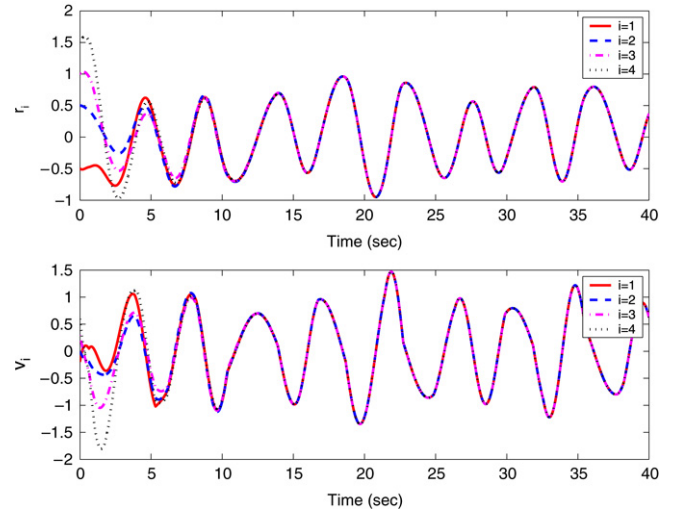


Fig. 7. Evolution of oscillator states over directed switching network topologies when $\alpha_{\sigma(t)}$ switches from (18) and $\mathcal{G}(t)$ switches from $\{\mathcal{G}_1, \mathcal{G}_2, \mathcal{G}_3\}$ as shown in Fig. 6.

Table 1
Parameters and initial conditions used in the simulation.

$\alpha = 1$
$\delta_{x1} = 0, \delta_{x2} = 4, \delta_{x3} = 0, \delta_{x4} = 4$
$\delta_{y1} = 0, \delta_{y2} = 0, \delta_{y3} = -4, \delta_{y4} = -4$
$x_0(0) = 1, x_1(0) = 1.2, x_2(0) = 0.8, x_3(0) = 1.4, x_4(0) = 0.5$
$y_0(0) = -1, y_1(0) = -1.2, y_2(0) = -0.8, y_3(0) = -0.7, y_4(0) = 1.5$
$v_{x0}(0) = 1, v_{x1}(0) = 0.2, v_{x2}(0) = 0.3, v_{x3}(0) = 0.4, v_{x4}(0) = 0.5$
$v_{y0}(0) = 1, v_{y1}(0) = 0.4, v_{y2}(0) = 0.6, v_{y3}(0) = 0.8, v_{y4}(0) = 1$

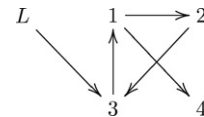


Fig. 8. Network topology for the four agents and the virtual leader. An arrow from node j to node i denotes that agent i can receive information from agent j . An arrow from node L to node i denotes that agent i can receive information from the virtual leader.

where α is a positive constant. We apply (14) to design w_{xi} and w_{yi} , respectively, as

$$w_{xi} = -\alpha(x_i - \delta_{xi}) - \sum_{j=1}^n a_{ij}(v_{xi} - v_{xj}) - a_{i0}(v_{xi} - v_{x0})$$

$$w_{yi} = -\alpha(y_i - \delta_{yi}) - \sum_{j=1}^n a_{ij}(v_{yi} - v_{yj}) - a_{i0}(v_{yi} - v_{y0}),$$

where δ_{xi} and δ_{yi} are constant.

Parameters and initial conditions used in the simulation are shown in Table 1. By solving (19) with the initial conditions of the virtual leader shown in Table 1, it is straightforward to show that the trajectory of the virtual leader follows an elliptic orbit.

Fig. 8 shows the network topology for the four agents and the virtual leader. We let $a_{ij} = 1, i, j = 1, \dots, 4$, if agent i can receive information from agent j and $a_{ij} = 0$ otherwise. We also let $a_{i0} = 1, i = 1, \dots, 4$, if agent i can receive information from the virtual leader and $a_{i0} = 0$ otherwise.

Fig. 9 shows the complete trajectories and snapshots of the four agents. Note that the four agents are able to synchronize their motions and move on elliptic orbits.

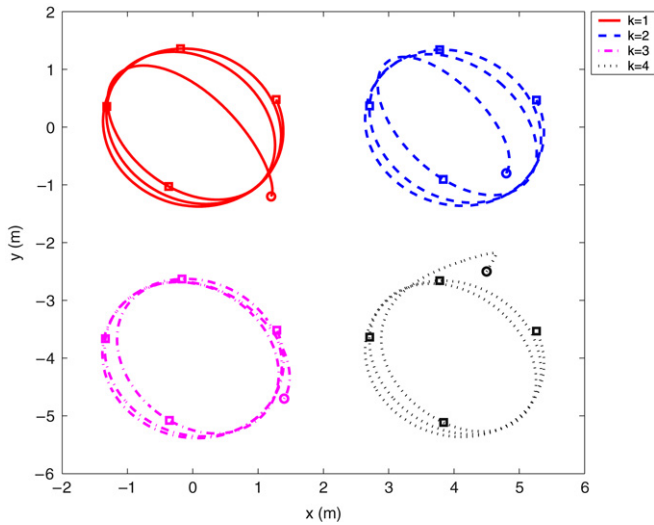


Fig. 9. Complete trajectories of the four agents. Circles show the snapshot at $t = 0$ s while squares show the snapshots at $t = 5, 10, 15, 20$ s.

6. Conclusion and future work

We have studied synchronization of coupled harmonic oscillators with local interaction. In the case of directed fixed network topologies, we have shown that the coupled second-order linear harmonic oscillators are synchronized when the directed network topology has a directed spanning tree. In the case of directed switching network topologies, we have shown that the coupled harmonic oscillators are synchronized when the directed network topology is strongly connected and balanced at each time instant or the directed network topology has a directed spanning tree at each time instant and the dwell time between switchings is sufficiently large. Examples have been given to validate the convergence conditions. The theoretical result has also been applied to synchronized motion coordination of multi-agent systems to show the effectiveness of the proposed strategy. In future work, we will apply the ideas in the current paper to cooperative scanning of an area with multiple robotic vehicles in experiments.

References

- Chopra, N., & Spong, M. W. (2005). On synchronization of Kuramoto oscillators. In *Proceedings of the IEEE conference on decision and control, and the European control conference* (pp. 3916–3922).
- Chopra, N., & Spong, M. W. (2006). Passivity-based control of multi-agent systems. In S. Kawamura, & M. Svinin (Eds.), *Advances in robot control: From everyday*

- physics to human-like movements* (pp. 107–134). Berlin: Springer-Verlag.
- Jadbabaie, A., Motee, N., & Barahona, M. (2004). On the stability of the Kuramoto model of coupled nonlinear oscillators. In *Proceedings of the American control conference* (pp. 4296–4301).
- Kuramoto, Y. (1984). *Chemical oscillations, waves and turbulence*. Berlin: Springer.
- Morse, A. S. (1996). Supervisory control of families of linear set-point controllers-part 1: Exact matching. *IEEE Transactions on Automatic Control*, 41(10), 1413–1431.
- Nijmeijer, H., & Rodriguez-Angeles, A. (2003). *Synchronization of mechanical systems*. Singapore: World Scientific.
- Olfati-Saber, R., Fax, J. A., & Murray, R. M. (2007). Consensus and cooperation in networked multi-agent systems. *Proceedings of the IEEE*, 95(1), 215–233.
- Olfati-Saber, R., & Murray, R. M. (2004). Consensus problems in networks of agents with switching topology and time-delays. *IEEE Transactions on Automatic Control*, 49(9), 1520–1533.
- Paley, D. A., Leonard, N. E., & Sepulchre, R. (2005). Oscillator models and collective motion: Splay state stabilization of self-propelled particles. In *Proceedings of the IEEE conference on decision and control, and the European control conference* (pp. 3935–3940).
- Paley, D. A., Leonard, N. E., & Sepulchre, R. (2006). Collective motion of self-propelled particles: Stabilizing symmetric formations on closed curves. In *Proceedings of the IEEE conference on decision and control* (pp. 5067–5072).
- Papachristodoulou, A., & Jadbabaie, A. (2005). Synchronization in oscillator networks: Switching topologies and non-homogeneous delays. In *Proceedings of the IEEE conference on decision and control, and the European control conference* (pp. 5692–5697).
- Ren, W., & Atkins, E. M. (2007). Distributed multi-vehicle coordinated control via local information exchange. *International Journal of Robust and Nonlinear Control*, 17(10–11), 1002–1033.
- Ren, W., & Beard, R. W. (2005). Consensus seeking in multiagent systems under dynamically changing interaction topologies. *IEEE Transactions on Automatic Control*, 50(5), 655–661.
- Ren, W., Beard, R. W., & Atkins, E. M. (2007). Information consensus in multivehicle cooperative control: Collective group behavior through local interaction. *IEEE Control Systems Magazine*, 27(2), 71–82.
- Ryan, E. P. (1998). An integral invariance principle for differential inclusions with applications in adaptive control. *SIAM Journal on Control and Optimization*, 36(3), 960–980.
- Tanner, H. G., Jadbabaie, A., & Pappas, G. J. (2007). Flocking in fixed and switching networks. *IEEE Transactions on Automatic Control*, 52(5), 863–868.
- Xie, G., & Wang, L. (2007). Consensus control for a class of networks of dynamic agents. *International Journal of Robust and Nonlinear Control*, 17(10–11), 941–959.



Wei Ren received the B.S. degree in Electrical Engineering from Hohai University, China, in 1997, the M.S. degree in Mechatronics from Tongji University, China, in 2000, and the Ph.D. degree in Electrical Engineering from Brigham Young University, Provo, UT, in 2004. From October 2004 to July 2005, he was a research associate in the Department of Aerospace Engineering at the University of Maryland, College Park, MD. Since August 2005, he has been an assistant professor in the Electrical and Computer Engineering Department at Utah State University, Logan, UT. His research focuses on cooperative control of multi-vehicle systems and autonomous control of unmanned vehicles. Dr. Ren is the co-author (with Randal Beard) of the book *Distributed Consensus in Multi-vehicle Cooperative Control* (Springer-Verlag, 2008). He was the recipient of a National Science Foundation CAREER award in 2008. He is currently an Associate Editor for the IEEE Control Systems Society Conference Editorial Board.